Explanation For the Dark I-V Curve of III-V Concentrator Solar Cells

Beatriz Galiana , Carlos Algora and Ignacio Rey-Stolle
Institute de Energia Solar, Universidad Politecnica de Madrid (IES-UPM), ETSI de Telecomunicacion, Avda. Complutense s/n, 28040 Madrid, Spain

The measurement of the dark I-V curve is one of the most straightforward methods for characterizing solar cells. Consequently, an accurate knowledge of its meaning is of high relevance for the comprehension and technological feedback of these devices. In this paper, an explanation of the dark I-V curve for concentrator III-V solar cells is presented using a 3D (three-dimensional) model in order to provide a proper data fit that provides meaningful physical parameters that are also compatible and coherent with a data fit from illumination curves. The influence on the dark I-V curve of the most significant series resistance components of concentrator solar cells is also analysed concluding that only the vertical component as well as the front contact-specific resistance can be assessable by means of this characterization method while both emitter and metal sheet resistances cannot be detected. For comparison purposes, the same experimental data have been fitted by means of a traditional two-diode model showing that, although an accurate dark I-V curve fitting can be achieved, the extracted parameters are unable to reproduce illumination data since lumped models assume the same ohmic losses distribution for both dark and illumination conditions.

KEY WORDS: modelling; concentrator solar cells; III-V compounds; dark I-V curve

INTRODUCTION

The dark behaviour of a solar cell has traditionally been modelled by means of an equivalent circuit consisting of a lumped series resistance *(R_S)*, a lumped shunt resistance *(R_P)* and a diode with an ideality factor ranging from 1 to 2. In most cases, the experimental data for III-V solar cells cannot be fitted properly using just one diode. Consequently, a two-diode model consisting of one diode with an ideality factor equal to 1 *(mi)* and one diode with an ideality factor equal to 2 *(m_2)* should be used whose equivalent circuit is shown in Figure 1 and it is described by:

$$I_{\mathrm{dark}} = I_{01} \cdot \left[\exp\left(q\frac{V + I_{\mathrm{dark}}R_{\mathrm{S}}}{m_1 kT}\right) - 1\right] + I_{02} \cdot \left[\exp\left(q\frac{V + I_{\mathrm{dark}}R_{\mathrm{S}}}{m_2 kT}\right) - 1\right] + \left(\frac{V + R_{\mathrm{S}}I_{\mathrm{dark}}}{R_{\mathrm{P}}}\right) \qquad (1)$$

Nevertheless, even using two diodes, most dark I-V curves can only be partially fitted by imposing values for mi and m_2 different from 1 and 2, respectively. This kind of fit provides a good mathematical fit but

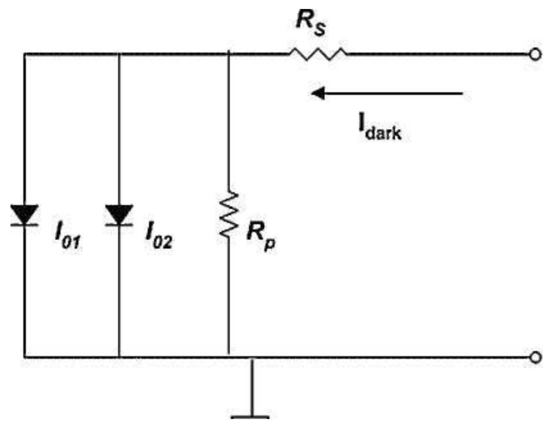

Figure 1. Two-diode lumped model for a single-junction solar cell in dark conditions

lacks a physical meaning since classic semiconductor theory regarding recombination mechanism in a p-n junction assumes two different types of recombination mechanism: the kT-recombination, that takes place in the neutral zones and the 2kT-recombination related to the space charge. For concentrator solar cells, the perimeter recombination is also very relevant and it also follows a 2kT-recombination. Consequently when the solar cell is modelled by means of two diodes, the ideality factors must be 1 and 2.

Additionally, the two-diode model is based on lumped parameters and assumes that the series resistance *(R_s)* and the shunt resistance *(R_P)* in the dark and under illumination are the same. In other words, in the two-diode model the lumped parameters should result in the same ohmic losses both with and without illumination. This simulation assumption is in opposition to the observed behaviour in concentrator solar cells. In fact, the resultant parameters extracted from the dark I-V curve and the illumination data disagree. Different strategies have been developed in order to fit dark and illumination data under different concentration levels. Some authors have proposed the variation of the ideality factor which implies different values for the inverse current saturation (7oi, /02) while others define a R_s value for dark conditions and a different R_s value for illumination conditions.

But, for a real III-V solar cell, the series resistance must be independent of the illumination level since some components, such as the emitter sheet resistance, are intrinsic properties of the solar cell, and others, such as the metal sheet resistance, are a consequence of the metallization procedure. On the other hand, concerning the recombination mechanisms, GaAs solar cells reach the high injection regime for illumination levels at around 5000X-10 000X. Consequently, the high injection regime is far from the actual operating conditions of concentrator solar cells. Then, for the viable concentration range, it can be assumed that $/_0$i and $/_0$2d m GaAs solar cells are also independent on the illumination level. But even though these parameters can be considered as constants, the influence of the series resistance components and the recombination mechanisms on the solar cell response vary with concentration. This is why some authors define a different ideality factor or R_s values depending on the illumination level.

Consequently, a more accurate model is required in order to provide fitting parameters that allow a proper data fit together with a reliable prediction of the solar cell response both in dark and under illumination (including concentration).

DISTRIBUTED MODEL

Accordingly, an explanation of the dark I-V curve is presented in this paper using a 3D network model based on distributed circuit units, that is, it does not resolve the continuity equations in 3D, but it does model the different current paths in a distributed manner. The model was previously presented and has already been successfully used for different applications. This model looks at all the loss effects (recombination, series resistance and shunt resistance) in a distributed manner by dividing the solar cell into elementary units (illumination, dark and perimeter) and assigning a specific circuit model to each one (Figure 2). With regard to the recombination mechanisms, three diodes are used: one for the neutral zone *(mi* = 1 and *J01),* one for the depletion region ($m_{2<}$j = 2 and /02a) and one for the perimeter (m_{2p} = 2 and /o2p)- For the ohmic losses in a single junction solar cell, the series resistance components are: the front contact specific resistance (PFC), the grid metal sheet resistance (r_{Msheet}), the vertical series resistance (r_v) which results from the vertical current flow (i.e. through the base, substrate and back contact) and the emitter sheet resistance (r_{Esheet}). Concerning the shunt resistance, two different origins are taken into account: the shunt resistance in the bulk device (r_P) and the shunt resistance at the perimeter (r_{P_per}). For small

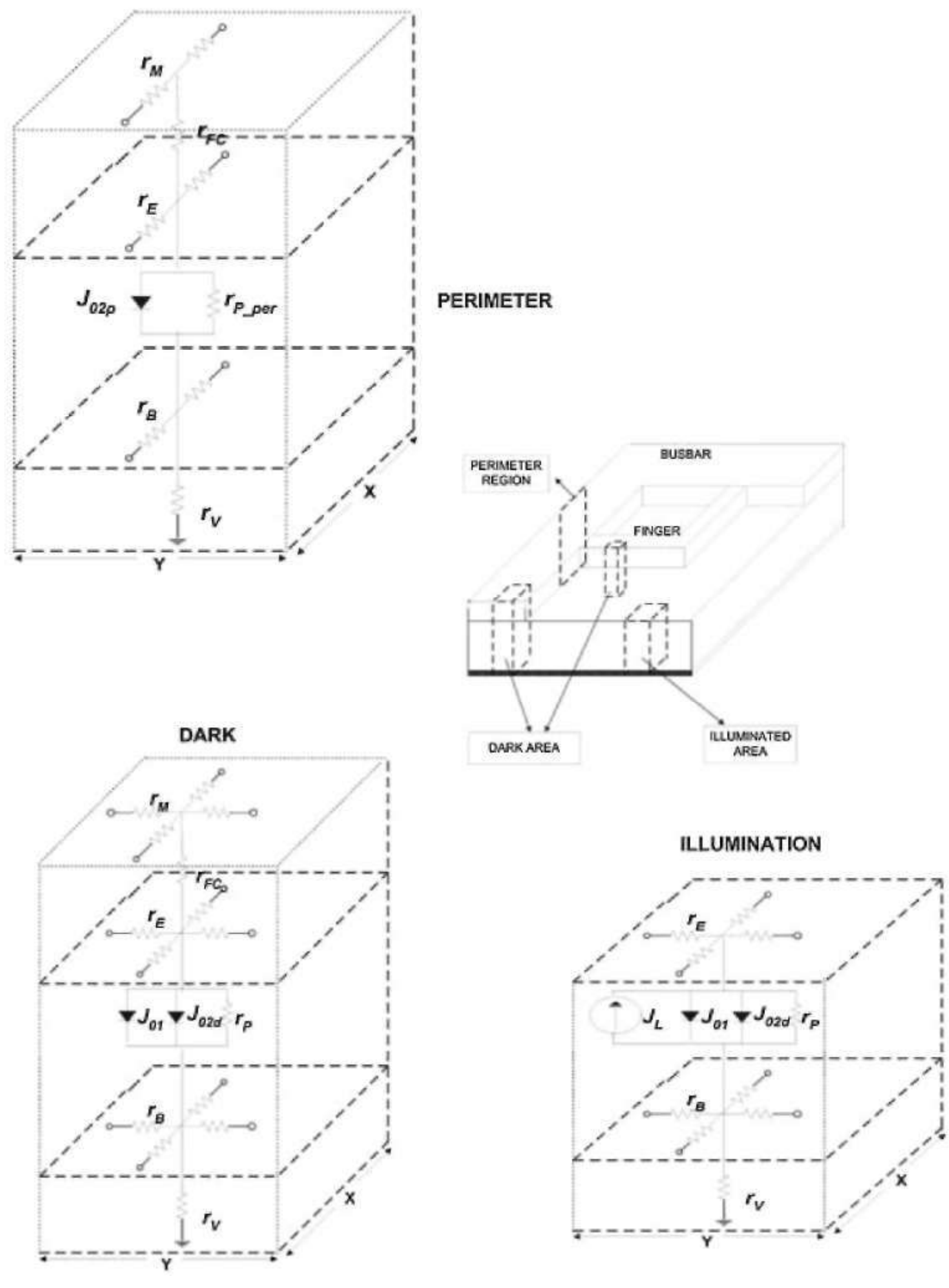

Figure 2. 3D network model for a single-junction solar cell showing the main elementary units

III-V concentrator solar cells the perimeter/area ratio is high and consequently the independent treatment of the shunt resistance at the perimeter and in the bulk is of great relevance for an accurate modelling. The different circuit units used in the 3D distributed model are presented in Figure 2 for a single junction device. It is important to bear in mind that different circuit units usually have different geometric dimensions *(X* and *Y* can be varied) and, consequently, the fit parameters are expressed per unit area, while in the two-diode model the extracted parameters are absolute. In fact, the most important restrictions concerning the dimensions of the circuit units of the 3D network model are the size of the fingers that must be smaller than the metal transfer length, and the size of the illumination circuit units that must be smaller than the minority carrier diffusion length in the emitter or the base.

EXPERIMENTAL

A concentrator GaAs solar cell has been analysed by means of the 3D network model and the two-diode model for dark and concentration conditions. The semiconductor structure of the solar cell has been grown on a p-type GaAs substrate (1 x 10 cm~) with the following layers: a 200 nm Alo.3Gao.7As BSF (5 x 10^{18}cm~^{3}), a 3.5 |Jim p-type base (2 x 10^{17}crrT^{3}), a 180 nm n-type emitter (1 x 10^{18}cm~^{3}) and a 25 nm GalnP window layer (1 10^{18}crrr^{3}). The front contact metallization is based on AuGe/Ni/Au and the back contact metallization is AuZn/Au. The solar cell active area is 1 mm^2 having an inverted square grid of 11 fingers of 3 *\xm* width with a pitch of 79 |Jim. The external busbar is 100 *\x,m* wide.

The dark I-V curve was measured using a temperature-controlled chuck once the solar cell was encapsulated on a copper heat sink for the back and with four external connections for the front. Measurements under concentrated illumination were also taken on the encapsulated solar cell using a flashlamp-based system with a measuring principle similar to the one described The main feature of this system is that the tracing of an I-V curve at a given concentration requires as many flashes as points on the I-V curve.

SIMULATION RESULTS

For this solar cell, the dark I-V curve has been fitted using both the 3D network model and the lumped two-diode model. For the 3D network model, only a quarter of the solar cell has been simulated for reasons of symmetry. In terms of circuit units, all the simulations have been carried out using a finger circuit unit of l x l |jLm, an illumination circuit unit of 5 x 5 |Jim, a perimeter circuit unit of 10 |Jim and a busbar circuit unit of 10 x 10|JLm. This implies that for a quarter, the number of circuit units is around 4000.

Agreement between experimental and theoretical dark I-V curve

In order to extract conclusions from the simulation results, the fit error for a fixed voltage (e_F) is defined by:

$$\varepsilon_F = \frac{I_{EXP} - I_{FIT}}{I_{EXP}} \cdot 100(\%)$$

where $/_E$xp is the experimental current for a fixed voltage and 7_{Frr} is the fit current for the same fixed voltage has been introduced in Figure 3.

In Figure 3, the resulting fit curves, the experimental data and the fit error are plotted. The parameters resulting from the fit are summarized in Table I. A more detailed description of the fit strategy can be found

A first conclusion that can be drawn is that by making mj equal to 1 and m_2 equal to 2, the 3D model fairly reproduces the experimental data, while the two-diode model differs at low voltages. This disagreement is because this I-V range has to be explained by means of shunt losses in the perimeter together with a bulk shunt resistance. If the perimeter effect is ignored, the 3D-network model is not able to achieve a good dark I-V curve fitting ('3D-network model without perimeter' in Figure 3) neither.

Illumination I-V curve calculation

Once the dark I-V curve (Figure 3) has been fitted, the extracted parameters have been corroborated using them to fit illumination curves for several concentrations with the 3D-network model and with the two-

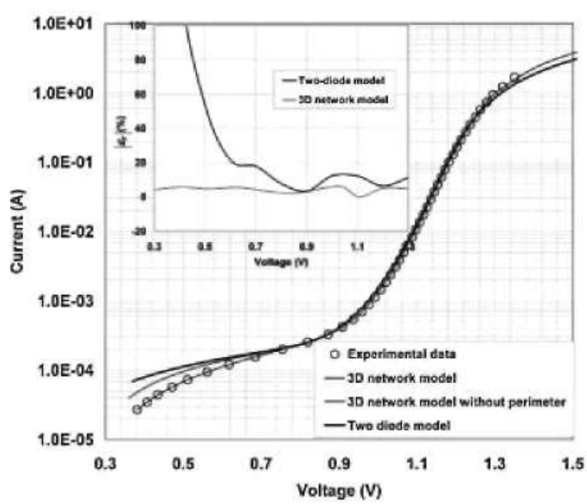

Figure 3. Experimental dark I-V curve of a GaAs concentrator solar cell. The thin solid black line corresponds to the data fit obtained using the 3D network model. The thick solid grey line corresponds to the data fit obtained using the 3D network model without perimeter effect. The thick solid black line corresponds to the data fit obtained using the two-diode model (Equation 1) assuming *mi* — 1 and $m_2 — 2$. Additionally, an inset of the fitting error versus voltage for the two models have been included

Table I. Parameters obtained from the experimental data fit of Figure 3 by the two-diode model and the 3D network model

	3D network model	Fixed two-diode model (dark I-V curve fit)	Fixed two-diode model (illumination fit)
J_{Ql} (A/cm^2)	1.2 x 1 0 " "	n/a	
$/_0$2d (A/cm^2)	0.9 x 10~^{12}	n/a	
$/_0$2p (A/cm)	6.0 x 10~^{12}	n/a	
/oi (A)	n/a	1.4 x 10"	1.4 x 10"
Ioi (A)	n/a	2.9 x 10"	4.6 x 10"
Pec (O-cm^2)	3 x 10~^{5}	n/a	
^Msheet	0.3*	n/a	
$r_{ES}hcct$ (fl/n)	250*	n/a	
r_v(Ii-cm^2)	5 x 10~^{5}	n/a	
Ss (mil)	n/a	70	290
R_P (O)	n/a	3000	7800
r_P (O•cm^2)	>1M!)	n/a	
^{r}P_per (ft-cm)	8000	n/a	

For the 3D network model only current densities (A/cm) as well as resistance per unit area (Ocm) are applicable since each circuit unit has its own size. All the fit parameters have been extracted from the dark I-V curve except for r_{MshM} and r_{Eshsst} that have been obtained from the illumination data fit in Figure 5. On the other hand, when using the two-diode model, $J_{02}d$ and $J_{02}d$ are not applicable since the model does not differentiate between the perimeter and depletion region recombination. Additionally, the parameters obtained from the illumination data fit of Figure 5 by the two-diode model are also included. Concerning the two-diode model, *Rp*, R_s, 7_0i and I_{02} have been obtained from the dark I-V curve fitting.

'Although Figure 6 shows that r_{Ms}heet and $r_{Esbcl>t}$ have no influence in the dark, these parameters have been obtained from the fit of the illumination curves,

n/a: not applicable.

diode model (Figure 4). As can be seen, the simulated efficiency for a wide range of concentrations obtained through the two-diode model using the parameters obtained from the dark I-V curve fit (Table I) is greatly overestimated for medium and high concentrations, while it is underestimated for low concentrations. This behaviour is a result of the lumped nature of the two-diode model that assumes that R_P (that mainly influences at low concentrations) and R_s (that mainly influences at middle and high concentrations) are the same in the dark and under illumination. In order to verify this hypothesis, the illumination data of Figure 4 has been fitted by means of the two-diode model. The resulting parameters are also shown in Table I. This table shows that the values of 7_0i and I_{02} are different depending on whether the fitting is carried out on the dark I-V curve or the illumination data. Concerning the ohmic losses, the value obtained for *Rs* from the illumination data fit is much higher than the value extracted from the dark I-V curve. That is, the value obtained for R_s from the fit of the dark I-V curve using the two-diode model is only a part of the R_s detected under illumination. On the other hand, the *Rp* value obtained from the illumination data fit is also higher than the value extracted from the dark I-V fit. This is because under illumination conditions the shunt resistance losses are smaller as result of many parallel current paths. This effect is also observable when the

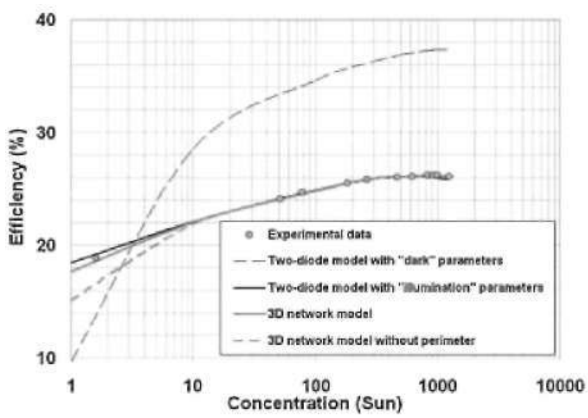

Figure 4. Efficiency as a function of concentration. The thick grey solid line corresponds to every concentration fit by means of the 3D network model using the parameters extracted from the dark I-V curve of Figure 4 ('3D network model'). The dashed black line corresponds to every concentration fit by means of the two-diode model using the parameters extracted from the dark I-V curve of Figure 4 ('Two-diode model with "dark" parameters'). The thick black solid line corresponds to every concentration fit by means of the two-diode model using different parameters than those obtained from the dark I-V curve fitting ('Two-diode model with "illumination" parameters'). The dashed grey line corresponds to every concentration fit by means of 3D network model neglecting the perimeter effect ('3D network model without perimeter').These parameters are summarized in Table I

perimeter effect is ignored in the 3D network model. If the dark I-V is fitting by the 3D model neglecting the perimeter effect ('3D network model without perimeter' in Figure 3) the resultant fitting values generate that at IX the efficiency is underestimated ('3D network model without perimeter' in Figure 4). This is because when the perimeter is ignored the r_p value required to fit the dark I-V curve of Figure 3 is much lower *(r_p* = 7500 il-cm^2) than when the perimeter is considered (r_p>l Mil-cm).

In contrast, the values of the series and shunt resistance components resulting from the dark I-V fit with the 3D network model allow an accurate description of the illuminated I-V curve, since this model allows alternative current paths through different resistances in parallel (see Figure 2) as actually happens in a real solar cell.

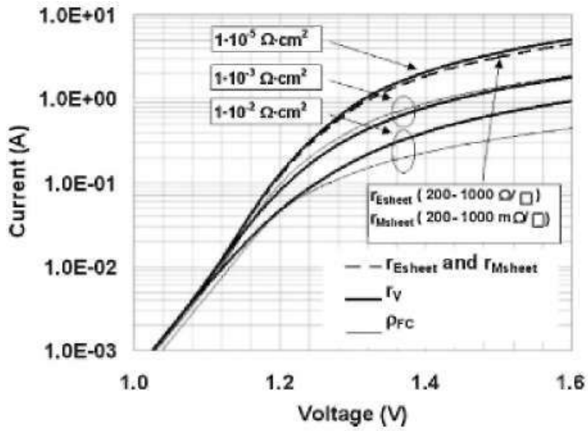

Figure 5. Simulated dark I-V curves obtained through the 3D network model with r_v varying from 1 x 1CF to 1 x l(T^{2}n-cm^2 and $p?_c$ from 1 x 1(T^5 to 1 x 10~^{2}fl-cm^2 Additionally, the simulation for f_{Esheet} equal to 200 and 1000 fl/n and for r_{Msheet} equal to 200 and lOOOmfl/D has been included (dashed black line)

DISCUSSION

In order to quantify the influence of the different series resistance components under dark conditions, the dark I-V curve has been simulated by the 3D network model varying different series resistance components (^{r}Esheet from 200 to 1000 *VLl* •, r_{Msheet} from 200 to 1000mn/rj, *ppc* and r_v from 1 x 10~^{5} to 1 x 10~ *fl-cm*) for a concentrator solar cell. In these cases, the influence of a given series resistance component has been obtained by fixing the other three series resistance components to their typical values for the state of the art of the technology (r_{Esheet} = 200 n/D, r_{Msheet} = 0.2fl/n, PFC = 5X 10^{-5} fl-cm^2 and r_v = 5 x 10~^{5} fl-cm^2). The first conclusion obtained from Figure 5 is that both the emitter sheet resistance (r_{Esheet}) and the metal sheet resistance (^{r}Msheet) have a negligible impact on the resulting dark I-V curves since, for any value, the resultant I-V curve is equivalent (dashed line in Figure 5). On the other hand, both the vertical resistance (r_v) and the front grid specific contact resistance *(ppc)* show a big influence under dark conditions. This effect is only visible by using a distributed model.

This conclusion implies that the dark I-V curve is of special relevance in detecting ohmic losses related to the vertical current flow (semiconductor structure, substrate and back contact and the front metal specific resistance), but no effect derived from the lateral current flow such as through the emitter or the metal sheet resistance is detected, although their influence under concentrated illumination is very important. Consequently, a concentrator solar cell could show a low series resistance in the dark but a very high ohmic losses under concentration, for example as a result of a high metal sheet resistance or emitter sheet resistance.

Additionally, the 3D network model allows the simulation of the voltage distribution on the solar cell surface. In Figure 6, a false greyscale map of the simulated voltage distribution of a GaAs single junction concentrator solar cell forward biased at 1.3 V is presented. The voltage and current density through the vertical resistance, r_v, of a cross section in the centre of the cell (white line) has been included in the Figure 6.

From Figure 6, it can be derived that the maximum voltage drop between the centre of the active area and the busbar region where the external wires are placed (each corner) is around 0.1 V (1.3V at the busbar and 1.2 V at the centre of the cell). In terms of current, this voltage drop means that the current flowing through the active area region is about one order of magnitude lower than the one through the external busbar (Figure 6). In fact, according to the experimental data of Figure 3 (dark I-V curve), the corresponding current for 1.3 V is 1 A. For a GaAs solar cell of 1.2 x 1.2 mm, the current density for 1.3 V is 69 A/cm^2. This reference value has been included in Figure 6 (dashed black line). As it can observed, only beneath the busbar region there are higher current densities than the reference value. This result shows also that in a dark I-V measurement, the current flow is

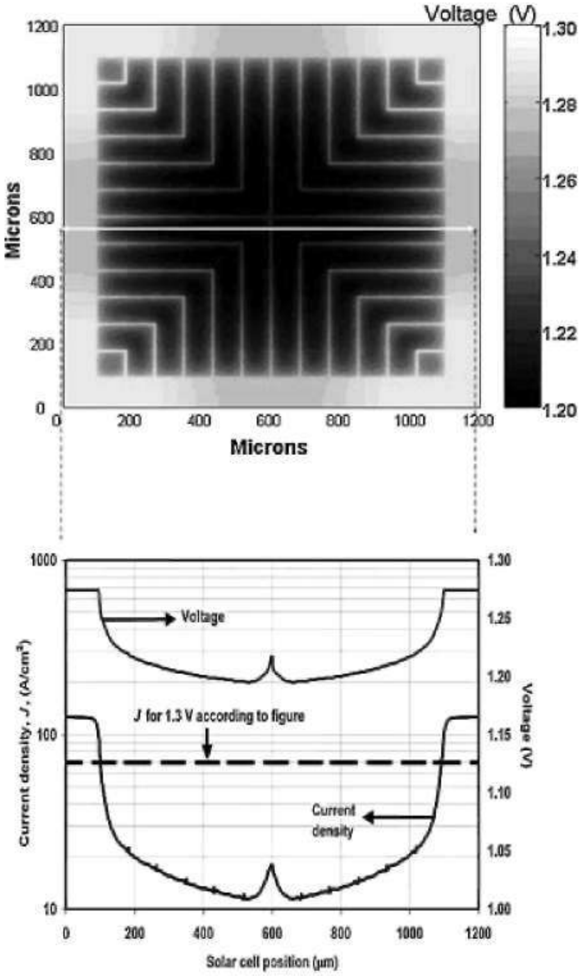

Figure 6. False grey scale map of the simulated voltage distribution under dark configuration for a bias polarization of 1.3 V at the four corners. Additionally, the voltage and density current has been calculated in a transversal section (white line in the greyscale map)

mainly vertical beneath the busbar and, consequently, only ry and *p^c* have influence, thus explaining the results discussed above. As a rule of thumb, the dark I-V curve only characterizes the solar cell portion beneath the busbar or metallization path where the external connections are placed for concentrator solar cell with a grid orientated for a point focus concentrator.

CONCLUSIONS

The main conclusions of this paper are, in first place, that even though the dark I-V curve of a concentrator solar cell could be fairly fitted by the two-diode model (equation 1), the extracted parameters are not compatible with the experimental data under illumination. But, by using a 3D network model, both the dark and the illumination data can be fitted with the same set of fitting parameters without any correction factor, being the first time that a good experimental fitting for dark and concentrated illumination data can be achieved with the same set of parameters.

In second place, the origin of the differences between the dark and illumination ohmic losses have also been presented, showing that the most important series resistance components for the dark I-V curve are those related to the vertical current flow such as, the vertical resistance (r_v) and the front contact-specific resistance *(ppc)*, while the emitter sheet resistance (^{r}Esheet) $^{a n}$d the metal sheet resistance (r_{Msheet}) have no influence on the dark I-V measurements, but they have a key role under concentrated illumination. This result is of special relevance to understand and extract reliable information from the dark I-V curve.

Finally, a voltage distribution in the dark is presented together with a density current in a transversal section of a GaAs solar cell, concluding that in a dark I-V measurement the current flowing through the active area region is about one order of magnitude lower than the one through the external busbar. This result reinforces the previous conclusion that only ry and *ppc* have influence in the dark I-V measurements.

Acknowledgements

This paper has been supported by the European Commission under contract SES6-CT-2003-502620 (FULLSPECTRUM project). The Spanish Ministerio de Educacion y Ciencia has also contributed with the CONSOLIDER-INGENIO 2010 programme by means of the GENESIS FV project and also with the research projects with references TEC2005-02745 and TEC2004-22300-E as well as the Comunidad de Madrid under NUMANCIA programme (S-505/ENE/0310). The authors would like to thank the reviewers their interesting comments and suggestions.

REFERENCES

Anton I, Sala G, Heasman K, Kern R, Bruton TM. Performance prediction of concentrator solar cells and modules from dark I-V characteristics. *Progress in*

Photovoltaics: Research and Applications 2003; 11(3): 165-178.

Vishnoi A, Gopal R, Dwivedi R, Srivastava SK. Distributed parameter analysis of dark I-V characteristics of the solar cell: estimation of equivalent lumped series resistance and diode quality factor. *Proceedings G IEEE of Circuits, Devices and Systems* 1993; 140(3): 155-164.

Algora C, Marti A, Araiijo GL. Characterization of the dark I-V curve of p/n GaAs heteroface solar cells. *Proceeding of the 8th photovoltaic solar energy conference,* 1988; 1512-1516.

Kaminski A, Marchand JJ, Fave A, Laugier A. New method of parameters extraction from dark I-V curve. *IEEE Photovoltaic Specialists Conference* 1997; 1: 203-206.

Haouari-Merbah M, Belhamel M, Tobias I, Ruiz JM. Method of extraction and analysis of solar cell parameters from the dark current-voltage curve. *Spanish Conference on Electron Devices* 2005; 2: 275-277.

Grove AS. *Physics and Technology of Semiconductor Devices*, Ed. John Wiley and Sons, 1967.

Henry CH, Logan RA, Merrit FR. The effect of surface recombination on current in AlxGa^xAs heterojunctions. *Journal of Applied Physics* 1978; 49(6): 3530-3542.

Araki K, Yamaguchi M. Extended distributed model for analysis of non-ideal concentrator operation. *Solar Energy Materials and Solar Cell* 2003; 75: 467^173.

Nielsen LD. Distributed series resistance effects in solar cells. *IEEE Transactions on Electron Devices* 1982; **ED-29:** 821-827.

Aberle AG, Wenham SR, Green MA. A new method for accurate measurements of the lumped series resistance of solar cells. *IEEE Photovoltaic Specialists Conference* 1993; 133-139. DOI: 10.1109/PVSC.1993.347065

Araujo GL, Cuevas A, Ruiz JM. The effect of distributed series resistance on the dark and illuminated current—voltage characteristics of solar cells. *IEEE Transactions on Electron Devices* 1986; 33(3): 391^01.

The voltage that needs to be applied to a pn^+ junction in order to reach the high injection regime $(V_{H}i)$ is Vm — $2 Y^{m}$ $(-f^4)$ > where NA is the doping level of the p side and n_t is the intrinsic concentration of the semiconductor [GL: Araujo, G. Sala, J.M. Ruiz, "Fisica de los dispositivitos electronicos", ETSIT, 1980, ISBN: 84-7402-1002-2]. For a typical GaAs concentrator solar cell, NA is between 2-10 and 1-10 cm~ thus obtaining 1.281 V < V_{HI} < 1.361 V Taking into account that $V_{H!}$ is the voltage applied at the pn junction (so ohmic losses must be considered), illumination concentrations between 5000X and 1000X are required.

Galiana B, Algora C, Rey-Stolle I, Vara IG. A 3-D model for concentrator solar cells based on distributed circuit units. *IEEE Transactions on Electron Devices* 2005; 52(12): 2552-2558.

Gonzalez JR, Rey-Stolle I, Algora C, Galiana B. Microplasma breakdown in high-concentration III-V solar cells. *IEEE Electron Device Letters* 2005; 26(12): 867-869.

Galiana B, Rey-Stolle I, Algora C. Comparison of ID and 3D analysis of the front contact influence on GaAs concentrator solar cell performance. *Solar Energy Materials and Solar Cells* 2006; 90(16): 2589-2604.

Williams RE. *Modern GaAs processing methods.* Artech House, Boston-EE.UU, 1990.

Keogh W, Cuevas A. Simple Flashlam pTesting of Solar Cells. *Proceedings of the 26th IEEE Photovoltaic Specialists Conference* 1997; 199-202.